UNCERTAINTY IN CALIBRATING FLOOD PROPAGATION MODELS WITH FLOOD BOUNDARIES DERIVED FROM SYNTHETIC APERTURE RADAR IMAGERY

P. Matgen [a, *], J-B. Henry [b], F. Pappenberger [c], P. de Fraipont [b], L. Hoffmann [a], L. Pfister [a]

[a] Centre de Recherche Public – Gabriel Lippmann (CRP-GL), L-1511 Luxembourg, Luxembourg – matgen@crpgl.lu
[b] Service Régional de Traitement d'Image et de Télédétection (SERTIT), Parc d'Innovation, Bld S. Brant, BP 10413, F-67412 Illkirch Cedex, France – jb@sertit.u-strasbg.fr
[c] Joint Research Centre of the European Commission (JRC), Weather Driven Natural Hazards, IES, JRC, Italy – f.pappenberger@lancaster.ac.uk

KEY WORDS: Remote Sensing, Floods, Classification, Calibration, SAR, Performance, Fuzzy Logic

ABSTRACT:

An instantaneous synthetic aperture radar (SAR) derived flood extent map helps retrieving the distributed conveyance parameters in one-dimensional flood routing models. These models are generally calibrated based on the sole use of ground data. This research aims to use earth observation (EO) data in order to establish a significant parameter retrieval strategy, providing an alternative model calibration technique. Owing to model structural errors, parameter equifinality and the fuzziness of the available radar and ground data used for calibration, there are some uncertainties with respect to the model predictions. In order to assess these uncertainties in a statistical framework, Monte Carlo simulations of a well-documented flood event in the Alzette river floodplain, Luxembourg are used to explore the parameter space of roughness coefficients. It is shown that many parameter sets perform equally well. The subsequent generalized likelihood uncertainty estimation (GLUE) methodology is used to compare both calibration strategies. Due to the coarse resolution of the available radar scenes and the difficulty in defining an appropriate radar backscattering threshold value during the inundation delineation, the exact flood extent is relatively uncertain. Hence, it is recommended to use a fuzzy-rule based calibration procedure with the available instantaneous flood boundaries derived from ERS and Envisat radar scenes. The uncertainty bounds of the flood extension predictions are assessed for the two types of calibration procedures based on ground survey data and earth observation data respectively. It is shown that both techniques provide similar performances. By combining EO data with ground based data in the calibration procedure, the parameter space will be constrained providing more reliable flood extension predictions i.e. with narrower uncertainty bounds. This study shows that earth observation data are very useful for hydraulic model calibration and that their combined use with ground data provides more accurate inundation simulations.

1. INTRODUCTION

Despite the physical appeal of the river flow computations in hydraulic flood propagation models, calibration remains a compulsory stage in inundation modelling. Elevations of high water marks and aerial photography are the most commonly used ground data during model calibration. Due to its large footprint, its all weather, day and night capabilities, the synthetic aperture radar (SAR) imagery shows considerable advantages over these ground data as well as over remotely sensed data obtained by sensors operating at visible wavelengths. Maps of flooded areas can be obtained very quickly and at low cost. Moreover, the sparseness of punctual ground data often hampers the calibration and evaluation of distributed roughness parameters in hydraulic models. Hence, the main objective of this study is to establish a parameter retrieval strategy based on SAR data, thus providing an alternative model calibration technique that will be compared to the more common one based on traditional mapping methods.

As pointed out by Aronica et al. (1998), the application of a fuzzy rule based calibration technique along with a generalized likelihood uncertainty estimation (GLUE) procedure constitutes a new paradigm in the way we interpret the predictions of physically based models (see also Romanowicz and Beven,

2003). Many different parameter values give rise to almost equivalent model simulations in terms of performance measures related to the different reference data, a phenomenon commonly termed equifinality (Beven, 1993). In fact, potential error sources are numerous in hydraulic modelling (model uncertainty, parameter uncertainty, error in observed data) and no set of calibrated parameters enables an entirely successful simulation of all state variables at each stage of the flood event. However, the uncertainties of the predicted spatially distributed flood extent can be reduced when combining objective functions based on different types of observations available after the flood event. The uncertainty reduction by introducing multi-response data describing several aspects of the modelled system has been widely explored in recent years (Freer et al., 2004).

However, in the past only a few studies have investigated the potential use of earth observation data in model calibration (see for instance Horritt et al., 2001). This is why we intend in this study to find out if the inclusion of further earth observations, which the model is required to replicate, can ultimately lead to a significant reduction of uncertainties related to the model predictions.

---

* Corresponding author.

2. THE STUDY SITE AND THE AVAILABLE DATA

A flood prone area of the river Alzette, approximately 10 km in length, is selected as test site for this research. The selected river reach with its surrounding villages has been subject to severe flooding in the past. A well documented medium sized flood event in January 2003, with an estimated return period of 5 years, was used in this study. The available database comprises pre-flood and flood SAR images, continuous discharge measurements upstream and downstream of the river reach, surveyed high water marks and GPS control points of the maximum flood extent. A set of photographs taken during the flooding event is also available. Acquired during the rising limb and at the peak discharge respectively, two ERS-2 SAR and Envisat ASAR scenes cover the flooded area at two distinct stages of the event (Figure 1). Except for two markedly wide alluvial plains upstream and downstream of Luxembourg-city (one of these figures as test site in this study), the Alzette river flows through a narrow valley system, making it impossible to use earth observation data to delineate the flood extension conveniently.
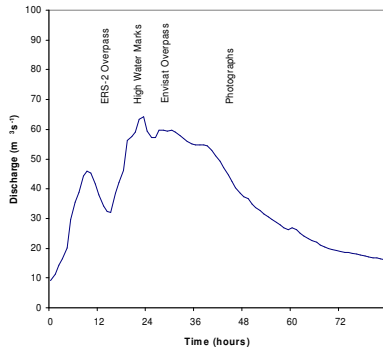

Figure 1. Upstream hydrograph for the 2003 flood event. The satellite overpass times are indicated. The high water marks correspond to the peak flow.

2.1 Pre-processing

The SAR instrument on board of the ERS-2 satellite is a C band (5.3 GHz) radar, operating in VV polarization with a spatial resolution of 30 m and a pixel size of 12.5 m (ESA, 1992). The Envisat satellite offers the ASAR instrument that enables to acquire data with alternate polarisation (AP). The combination of like- and cross-polarisations provides increased capabilities for flood mapping (Henry et al., 2003). In this study, the AP SAR data were acquired with a VV and VH polarisation combination. Among the three available radar scenes, the VH polarisation in the AP precision image allowed the best differentiation of "flooded" and "non-flooded" areas.

The radar data are first radiometrically calibrated and then orthorectified using a 75 m resolution DEM. The internal geometric coherence is evaluated at 1-2 pixels, i.e. the horizontal shift between any two images never exceeds this value. The calibration procedure used in this study to calculate the backscattering coefficient is based on Laur et al. (1998). Speckle noise is reduced using the Frost filtering with a 5 x 5 moving average filter.

3. METHODS

3.1 Flood boundary delineation using radar imagery

Due to the specular backscattering on plain water surfaces and the resulting low signal return, the flood mapping through SAR is quite straightforward. However, in the transient shallow water zone between the flooded and the non-flooded part of the floodplain (with protruding vegetation producing increased signal returns), the radar signal only gradually increases, thus making the accurate delineation of the flood boundary more difficult. Hence, a rather arbitrary choice of a backscattering threshold value is needed during the automatic binary segmentation of flooded/unflooded areas of the radar scene. Because of the poorly defined flood boundaries it is therefore highly recommended to use a fuzzy rule based calibration technique as a general approach to hydraulic modelling with uncertain data derived from earth observation data. Wind roughening is also a well known effect that eventually has to be taken into account. Despite these limitations, the use of SAR imagery compares favourably with other remote sensing systems (Biggin and Blyth 1996). In a case study Horritt et al. (2001) found that, despite the aforementioned limitations, the SAR segmentation algorithm classified 70 % of the SAR shoreline within 20 m of the shoreline as derived from aerial photographic data.

Because of the lack of standardised, reproducible methods (De Roo et al., 1999), a rather simplistic threshold approach was used in this study to obtain the inundation maps from the two available radar scenes. Therefore, profiles of pixel values at several cross sections of the river floodplain are drawn and confronted with the GPS control points of the maximum lateral flood extent. Thus, threshold values of radar backscattering are determined and used to classify the radar image as "flooded" and "non-flooded" respectively. As this raw classification method does not provide entirely satisfying results, three probability classes were defined reflecting the lack of knowledge about the "real" flood extent in the whole area (Figures 2 3). At each cross section the coordinates of the extension with high, intermediate and low probability of flooding are defined. Therefore, in a next section, a fuzzy performance measure will be defined that at each cross section reflects the uncertainties in the maximum flood extension as derived from the radar data.
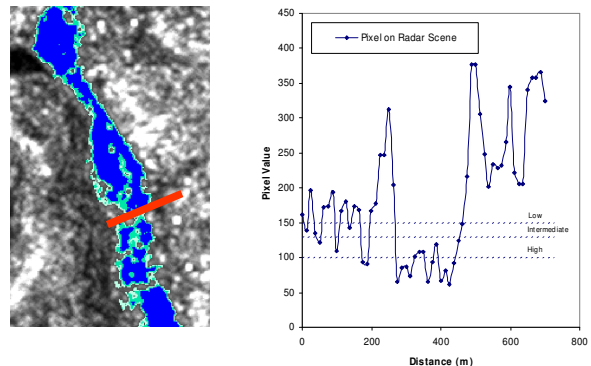

Figure 2. Spectral profile across a river transect

The resulting classified image (Figure 3) shows several flooded areas that are not directly connected to the riverbed. These patterns can be explained by surface runoff, groundwater

resurgence or misclassified pixels of the SAR imagery. The latter can be partially removed after confronting the classified image with photographs taken during the event. A further evaluation of the flood map can be achieved by combining the resulting image with a high resolution digital elevation model in order to derive the water elevation at each cross section. By comparing the profile of the water line with the elevation of the river bed, doubtful values can be outlined and eventually be removed from the reference data used during calibration.
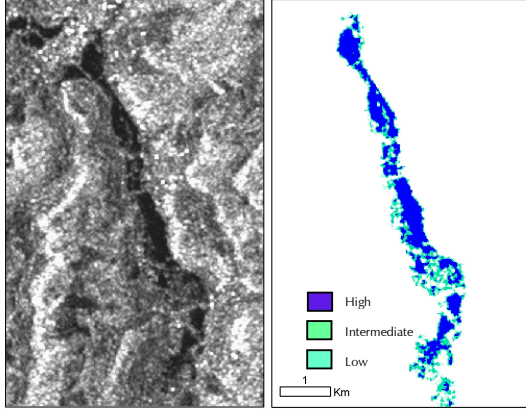

Figure 3. Three probability classes of flooding are defined

3.2 Flood propagation modelling

It is nowadays commonly accepted that, once riverbank overtopping occurs, river flow becomes two-dimensional. As 2D inundation models become more readily available, the calibration based on flood maps derived from earth observation data will become more popular. It is somewhat surprising that despite the obvious limitations in 1D model formulation, it has been shown that in some river reaches simple 1D models and the more sophisticated 2D models performed equally well (Horritt and Bates, 2002). Computational advantages therefore suggest that 1D models should be used whenever the topography of the floodplain allows considering the 1D river flow hypotheses.

The widely used 1D HEC-RAS model is used in the present study. This model requires a minimal amount of input data and computer resources and is thus very easy to use. The unsteady flow model UNET, which is part of HEC-RAS, solves the full 1D St Venant equations for unsteady open channel flow. The required input data comprises the topographical description of adjacent river and floodplain cross sections, the dimensions of hydraulic structures and the boundary conditions at the upstream and downstream end of the river reach. The description of the flood propagation is based on the commonly used Manning-Strickler formula which means that three roughnesses (one for the channel and two for the floodplains) are the free parameters that need to be calibrated in order to minimise the difference between simulations and observations. Nearly all one-dimensional and quasi two-dimensional flood propagation models use Manning's equation to estimate empirically the friction slope (Pappenberger et al., in press).

Downstream of Luxembourg-city, the HEC-RAS model was set up using 74 cross-sections that describe the channel and floodplain geometry. These data are extracted in GIS based on a high resolution, high accuracy DEM. The latter was obtained by combining the data describing the ground surveyed cross-sections and the floodplain data obtained by airborne laser altimetry. The inflow hydrograph of the January 2003 flood event constitutes the upstream boundary. At the downstream end of the river reach, the friction slope is set to the average channel slope. Assuming normal flow, the Manning equation then allows calculating for each time step the water height which is used as downstream boundary condition.

Nowadays, connections between 1D hydraulic models and Geographical Information Systems (GIS) allow for the accurate 2D mapping of simulated inundations. Hence, the comparison of these modelled flood extents with remotely sensed flood areas has become straightforward. However, the needed export of the model results into GIS makes that this remains a very time consuming task. As a matter of fact, in the present study, where a large number of computational runs were carried out, the distributed 2D inundation data are therefore processed in order to become compatible with 1D model calibration and evaluation. Therefore, the x and y coordinates at the intersection of the digitised flood boundary and each of the river cross sections considered in the model formulation, are extracted in the GIS environment. Next, for each model run and at each cross section, the distance between the simulated and the radar derived flood extent is computed and used to determine the likelihood of the underlying parameter set. Point measurements of stage and travel time do not need to be transformed prior to 1D model calibration and evaluation.

3.3 Model calibration

Remote sensing data sets (ERS-2 SAR and Envisat ASAR) and high water marks are used for calibration. These reference data have in common that they are relatively uncertain. Hence, fuzzy measures are most appropriate to reflect this noise in the data sets. The only condition a fuzzy membership function describing the likelihood of a given parameter set must satisfy is that it must vary between 0 and 1 (Freer at al., 2004). At those cross sections where high water marks are available, a fuzzy product definition of the performance measure (PM) was used, having the following form of trapezoidal membership function (Equation 1):

$$L[M(\Theta|Y_T, W_T)] = \prod_{i=1}^{n} \begin{cases} 0, & x \leq a \\ \frac{x-a}{b-a}, a \leq x \leq b \\ 1, & b \leq x \leq c \\ \frac{d-x}{d-c}, c \leq x \leq d \\ 0, & d \leq x \end{cases} \tag{1}$$

where $M(\Theta|Y_T, W_T)$ indicates the model, conditioned on input data Y_T and observations W_T. For each cross section i, x is the distance between the simulated water level and the surveyed high water mark. The parameters a, b (in this study -0.5 and 0.5 meters) define the core and the parameters c, d (in this study -1.5 and 1.5 meters) define the support of the trapezoidal membership function. The core defines the range of simulated water levels where the parameter set is credited with the highest possible likelihood value. The support is the range of water levels where we have a non-zero membership value. The performance measure of this model is given by the product of n fuzzy measures (n is the number of cross sections where HW is available). The maximum possible PM is 1.

Similar PMs are used with the radar data. The difference with the elevation data is that the parameters of the fuzzy membership function are now varying in space in order to take into account the individual inundation probability classes at each cross section (Figure 3). A custom PM was used, having the following form of membership function (Equation 2):

$$
L[M(\Theta|Y_T,W_T)]=\sum_{i=1}^{n}
\begin{cases}
0, & d\le-d_{weak}\\
\dfrac{L_{strong}(d+d_{weak})}{(d_{weak}-(res/2))}, & -d_{weak}<d<(-res/2)\\
L_{strong}, & (-res/2)\le d\le(res/2)\\
\dfrac{(L_{medium}-L_{strong})(d-res/2)}{d_{medium}-res}+L_{strong}, & (res/2)<d<d_{medium}-(res/2)\\
L_{medium}, & d_{medium}-(res/2)\le d\le d_{medium}+(res/2)\\
\dfrac{(L_{weak}-L_{medium})(d-d_{mery}-res/2)}{d_{weak}-d_{medium}-res}+L_{medium}, & d_{medium}+(res/2)<d<d_{weak}-(res/2)\\
L_{weak}, & d_{weak}-(res/2)\le d\le d_{weak}+(res/2)\\
0, & d_{weak}+(res/2)<d
\end{cases}
\quad(2)
$$

For each cross section i, d is the distance between the simulated water extent and the surveyed flood boundary of the highest probability class. The parameters L_{strong}, L_{medium} and L_{weak} are the membership values of the corresponding probability classes (1, 0.75 and 0.25 respectively). The resolution of the radar scene is taken into account with the parameter *res*. A fuzzy additive performance measure is used with each radar derived flood boundary. A multiplicative combination of PMs at each cross section would lead to the rejection of all models. These equations define a custom fuzzy membership set for the simulated flood extents (Figure 4).
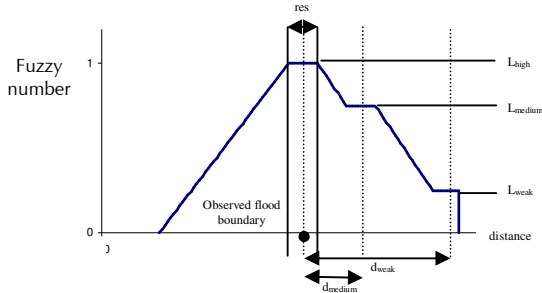

Figure 4. Fuzzy number used in this study

3.4 Generalized Likelihood Uncertainty Estimation (GLUE)

The GLUE procedure is a Bayesian Monte Carlo based technique, which allows for the concept of equifinality in the evaluation of modelling uncertainty (Beven, 1993). This approach is recommended in inundation modelling, because it rejects the concept of optimal models in favour of multiple behavioural models. In our study, the GLUE prediction limits are conditional probabilities of the simulated flood extent at each river cross section, which are conditioned on the choice of the model and the errors in both radar and ground based data.

First, a uniform sampling strategy is employed within user defined *a priori* feasible parameter ranges. A large number of simulation runs are required to sample the plausible parameter space adequately. As this research intends to assess multi-objective variations in the model performance within a GLUE framework, the results of each run are compared to the calibration data presented in the preceding section. Hence, the multi-objective data that the model should be able to replicate, are the surveyed high water marks (HW) and the flood

boundaries derived from the two radar data sets. Next, the user needs to define acceptable performance measures that will discriminate between "non-behavioural" and "behavioural" model runs, i.e. parameter sets that reproduce satisfactorily the observed hydrometric and inundation data respectively. The behavioural criteria for the multiple objectives are given in Table 1.

Performance measure	Equation	Acceptability Criteria
HW fuzzy product	Equation 1	0.8 (maximum possible = 1)
Envisat fuzzy additive	Equation 2	56 (maximum possible = 118)
ERS fuzzy additive	Equation 2	40 (maximum possible = 90)

Table 1. Performance measures and their acceptability criteria

These threshold PM values are used to reject the simulations that deviate too much from the observations. Because of the subjective choice of the discriminating rejection criteria, this method has been criticized in the past (Gupta et al., 1998) Therefore, a null-information model is calculated first. At the time of the satellite overpasses and during peak flow, the available continuous stage measurements at the boundaries of the river reach and at the intermediate bridges are linearly interpolated. The resulting flood map is used to calculate the three performance measures. A "behavioural" hydraulic model should perform better than this simplified mapping method and, consequently, these PMs are used as acceptability criteria during the further research (Table 1).

The likelihoods of the remaining behavioural model runs are re-scaled to sum unity. At the end of this procedure, these results are used to form likelihood-weighted cumulative distribution functions of the simulated water levels at each river cross section. The uncertainty quantiles of each cross section are linearly interpolated to produce percentile inundation maps for the whole area. The focus of this study being the parameter uncertainty, this GLUE analysis is performed with the effective channel and floodplain roughness coefficients. The latter should not to be mixed with the real physical parameters as the effective parameters may compensate for uncertainties in the topographical description and/or the discharge measurements, both of which are not individually assessed in this study.

4. RESULTS AND DISCUSSION

In total 22000 runs of the model with randomly chosen roughness coefficients (from a uniform distribution between 0.001 and 0.2) were generated. However, numerical instabilities that occurred with many parameter sets lead to the rejection by the model itself of almost half of them. These instabilities may be associated to many possible origins (Pappenberger et al., 2004). Finally 11608 initial sets remain for the further analysis. For each run, different performance measures were calculated. The dotty plots in Figure 5 represent a projection of the parameter space into 1 dimension. Each dot represents the objective associated with a single parameter set. Each column is associated with one of the 3 parameters considered in the hydraulic model: channel roughness, left and right floodplain roughness. These plots are presented for the three performance measures that were considered in this study: high water marks (HW), flood boundaries derived from ERS SAR and ENVISAT ASAR respectively. The performance measures in Figure 5 are a multiplicative combination of the HW PMs and an additive combination of the ERS and Envisat PMs at each river cross section.
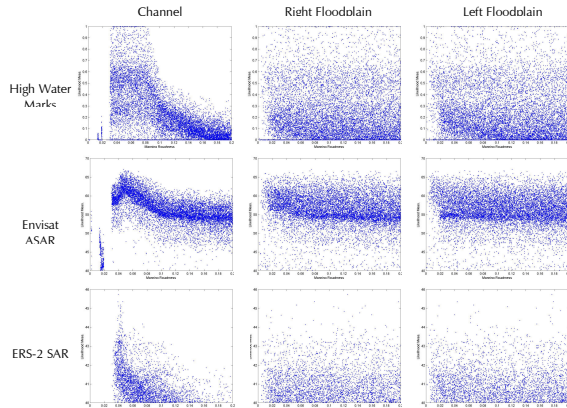
Figure 5 Dotty plots of parameter distributions for the different PMs

Obviously, a large number of parameter sets perform almost equally well. It is shown that the model performance mainly depends on the channel roughness coefficients whereas the model only shows limited sensitivity for the two floodplain friction parameters. Depending on the choice of the channel roughness, good fits can be achieved in the whole range of the sampled parameter values. In particular, a maximum likelihood value of 1 could be obtained for many different roughnesses in respect with the measured high water marks. The dotty plots also show that a considerable range of performance measures are produced inside the sampled parameter range. Clearly, some of these parameter sets produce output that has to be considered to be non-behavioural, i.e. the response deviates so far from the observations that the model cannot be considered as an adequate representation of the system. The parameter spaces of the simulations meeting the behaviourability criteria (Table 2) have only the channel roughness parameter constrained to its lower range from the initial sampling limits. The total number of behavioural simulations for each objective is given in Table 2. The dotty plots associated to each one of these objectives show the consistencies of the results and the friction parameters were more or less stationary between the two considered flood stages. With only 286 behavioural parameter sets remaining, the most important reduction of parameter sets is achieved with the HW criteria. As these data are the most reliable, a relatively high threshold PM value can be chosen. The fuzziness of the radar data hampers the use of higher threshold PM values.

	Behavioural simulations*	
Acceptability criteria	Total number	
HW	286	
Envisat	3926	
ERS	4542	
HW & Envisat	212	
HW & ERS	143	
HW & Envisat & ERS	**140**	

* Total number of simulations was 22000

Table 2. Behavioural simulations for indivual and combined PMs

The effect of combining different PMs is shown in Table 2. Only parameter sets meeting the behaviourability criterium of each one of the multiple objectives are retained in the final sample. Clearly, the number of behavioural simulations is considerably reduced. More than half of the 286 selected parameter sets are rejected based on the additional criteria and finally only 140 among the initial 22000 runs are considered as behavioural. Most notably, the additional ERS PM constrains

the model response most. This is not surprising as the ERS picture was taken during the rising limb preceding by several hours the peak discharge whereas the Envisat picture was taken close to peak discharge. Hence, the flood data derived from Envisat is somewhat redundant to the high water marks and the resulting parameter constrain is not noteworthy.
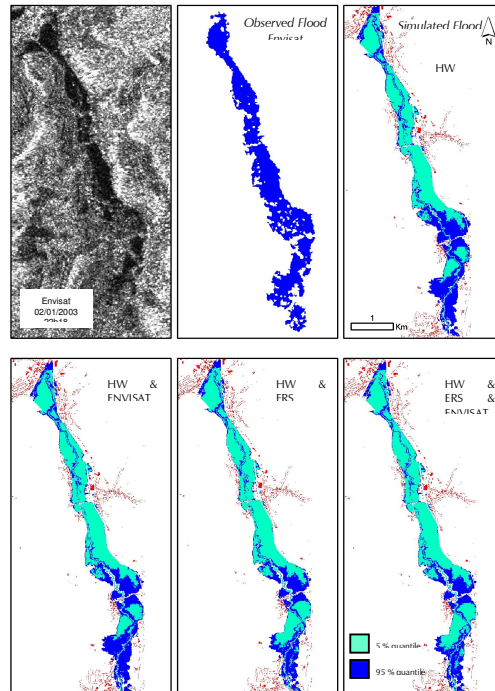
Envisat 02/01/2003 22h18

Figure 6. Updated 5% and 95% percentile inundation maps for behavioural simulations of individual and combined PMs (Envisat overpass time)

The progressive constraining of the model predictions by incorporating the additional Envisat radar data is also shown on Figure 6 with the distance between the boundary limits of the 5% and 95% quantile flood maps gradually narrowing. This means that simulations conditioned using all the PMs show smaller ranges of model behaviours than models conditioned only using the ground data. Only locally, for instance at the upstream end of the river reach, some major uncertainties subsist. The uncertainty maps based on the final parameter set constrained using all 4 PMs of Table 1 give inundation maps at peak discharge that are very close to what was observed by Envisat at the same time (Figure 7). Most importantly the range of simulated flood boundaries generally brackets the observed extents. It is not surprising that the uncertainty reduction by incorporating additional distributed radar data becomes most effective in those areas of the floodplain where surveyed point data are missing. The resulting uncertainties tend to be higher at an initial stage of the flood (during ERS-2 overpass). This may be due to changing roughness values with increasing water levels that lead to some doubtful parameter values being included and some good sets being rejected when considering high water marks only. Moreover, at a preliminary stage of the flood, small changes of the channel roughness coefficient may have a large impact on the simulated extent. This is due to the fact that when the river channel is bankfull, small changes of the water level tend to induce large changes of the flood extent. By

incorporating the ERS objective, the subsequent parameter constrain becomes visible in some areas.

5. CONCLUSION

The findings in this flood propagation study showed the equifinality of roughness coefficients and outlined the need for multi-response evaluation. Most importantly, it was shown that simulations calibrated with radar data performed almost equally well than the models only conditioned on ground data. The main difference between both calibration methodologies can be related to the increased fuzziness of earth observation data that leads to larger prediction uncertainties. Due to this redundancy, the responses of models that were initially conditioned using measured high water marks could not be significantly constrained with synchronically obtained radar observations. This does not mean that on different sites with sparse ground data sets, the constrain could not become significant. On our test site, however, a significant constrain was only achieved with radar data sets obtained several hours before peak flow occurred. This suggests that in order to become complementary to existing ground data, the radar coverage should be different in time and/or space from the point data sets. This approach could also help addressing the well-known problem of changing roughness values with increasing water levels. However, if the time interval between available data sets is too long, this may lead to the rejection of all model simulations. Therefore, it will be interesting to investigate whether additional data sets of different flood events will further constrain the plausible parameter sets or, in contrast, will lead to the rejection of all simulations.
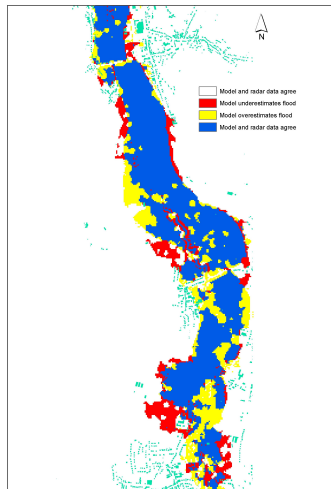

Figure 7. Comparison of the "best" simulation (based on radar observation) and the corresponding Envisat derived flood area

It has also been pointed out in this study that the application of a fuzzy rule based calibration technique, along with a generalized likelihood uncertainty estimation (GLUE) procedure, constitutes a valuable approach in inundation modelling. Fuzzy performance measures are perfectly suited for radar data with no knowledge of the error structure. Dealing this way with the most important sources of uncertainties could ultimately lead to an increase of confidence that flood managers will have in the simulation results.

6. REFERENCES

Aronica, G., Hankin, B., Beven, K.J., 1998. Uncertainty and equifinality in calibrating distributed roughness coefficients in a flood propagation model with limited data. *Advances in Water Resources*, 22(4), pp. 349-365.

Aronica, G., Bates, P.D., Horritt, M.S., 2002. Assessing the uncertainty in distributed model predictions using observed binary pattern information within GLUE. *Hydrological Processes*, 16, pp. 2001-2016.

Beven, K.J., 1993. Prophecy, reality and uncertainty in distributed hydrological modeling. *Advances in Water Resources*, 16(1), pp. 41-51.

Biggin, D.S., Blyth, K., 1996. A comparison of ERS-1 satellite radar and aerial photography for river flood mapping. *Journal of the Chartered Institute of Water Engineers and Managers*, 10, pp. 59-64.

De Roo, A., Van Der Knijff, J., Horritt, M., Schmuck, G., De Jong, S., 1999. Assessing flood damages of the 1997 Oder flood and the 1995 Meuse flood. *Proceedings of the 2nd International Symposium on Operationalization of Remote Sensing*, Enschede, The Netherlands.

Freer, J.E., McMillan, H., McDonnell, J.J., Beven, K.J., 2004. Constraining Dynamic Topmodel responses for imprecise water table information using fuzzy rule based performance measures. *Journal of Hydrology*,291(3-4), pp. 254-277.

Gupta, H.V., Sorooshian, S., Yapo, P.O., 1998. Toward improved calibration of hydrologic models: Multiple and noncommensurable measure of information. *Water Resources Research*. 34, pp. 751-763.

Henry, J.-B., Chastanet, P., Fellah, K., Desnos, Y.-L., 2003. ENVISAT Multi-Polarised ASAR data for flood mapping. *Proceedings of IGARSS'03*, Toulouse, France.

Horritt, M.S., Mason, D.C., Luckman, A.J., 2001. Flood boundary delineation from Synthetic Aperture Radar imagery using a statistical active contour model. *International Journal of Remote Sensing*, 22(13), pp. 2489-2507.

Horritt, M.S., Bates, P.D., 2002. Evaluation of 1D and 2D numerical models for predicting river flood inundation. *Journal of Hydrology*, 268, pp. 87-99.

Pappenberger, F., Beven, K.J., Horritt, M., Blazkova, S., 2004. Uncertainty in the calibration of effective roughness parameters in HEC-RAS using inundation data. *Journal of Hydrology*, in press.

Romanowicz, R., Beven, K.J., 2003. Estimation of flood inundation probabilities as conditioned on event inundation maps. *Water Resources Research*, 39(3): p. art. no.-1073.

7. ACKNOWLEDGEMENTS